Leaky surface acoustic waves in Z-LiNbO3 substrates with epitaxial AlN overlays

G. Bu, D. Ciplys, M. S. Shur, G. Namkoong, W. A. Doolittle et al.

Additional information on Appl. Phys. Lett.

Leaky surface acoustic waves in Z-LiNbO$_3$ substrates with epitaxial AlN overlays

G. Bu, D. Ciplys,[a] and M. S. Shur[b]
Department of Electrical, Computer, and Systems Engineering, Rensselaer Polytechnic Institute,
110 8th Street, Troy, New York 12180-3590

G. Namkoong, W. A. Doolittle, and W. D. Hunt
Georgia Institute of Technology, School of Electrical and Computer Engineering,
Microelectronic Research Center, 791 Atlantic Drive, Atlanta, Georgia 30332-0269

The properties of leaky surface acoustic waves (LSAW) in MBE grown AlN layer on Z-cut LiNbO$_3$ structures have been studied by numerical simulation and experimental measurements and compared with those of Rayleigh waves in the same structure. In the range of AlN layer thicknesses studied ($0 < kh < 0.145$) the measured velocity of LSAW propagating along the X axis of LiNbO$_3$ substrate was essentially constant at around 4400 m/s. The measured electromechanical coupling coefficients (K^2) for the LSAW are roughly 1/4 of the predicted values, which might be due to the strong attenuation of the leaky wave unaccounted for during the parameter extraction. The thin AlN film slightly improved the measured temperature coefficient of frequency for the LSAW over that attained for the Z-cut, X-propagating LiNbO$_3$ substrate alone. © *2004 American Institute of Physics*. [DOI: 10.1063/1.1805705]

Surface acoustic waves (SAW) devices have found numerous applications in communications and sensors. High SAW velocity, large electromechanical coupling coefficient, and good temperature stability are of importance for certain classes of practical SAW devices. In piezoelectric materials, these requirements are not typically satisfied simultaneously. For example, the cuts of LiNbO$_3$, widely used for wide bandwidth SAW devices, exhibit high electromechanical coupling coefficients, but feature moderate SAW velocities and poor temperature stability. However, certain cuts of aluminum nitride have considerably higher SAW velocities and better temperature stability, but the electromechanical coupling constants in AlN are typically lower than those obtained with LiNbO$_3$.[1,2] It is anticipated that the optimal trade-off between properties of both materials might be obtained using an AlN on LiNbO$_3$ layer-substrate structure. The Rayleigh-type surface acoustic wave properties in structures fabricated by rf magnetron sputtering of AlN films on Z-and Y-128° LiNbO$_3$ have been recently studied.[3–6] There is also much interest in studies and applications of other wave types, in particular, of the leaky surface acoustic waves (LSAW). It should be noted that Z-cut lithium niobate is not among the orientations commonly used for SAW devices. However, it is widely used in integrated optic applications. The leaky surface acoustic waves may be of interest for guided-wave acousto-optic interactions. Higher velocities of LSAW as compared to the Rayleigh-wave velocities are an advantage for achieving higher operation frequencies with the same photolithography-defined transducer dimensions. This is of particular concern as wireless protocols call for higher frequency front-end filters. Moreover, the leaky waves associated with Z-cut X-propagating LiNbO$_3$ are dominantly shear-polarized in the propagation plane and hence are suitable for liquid phase sensing. Shear horizontal plate waves in LiNbO$_3$ have been studied in Refs. 7 and 8. In this letter, we present the results of simulation and experimental investigation of leaky surface acoustic wave properties in epitaxial-AlN-film/ Z-LiNbO$_3$-substrate structures.

AlN was grown on Z-cut lithium niobate at 800 °C, using 0.32 sccm nitrogen, at 0.4 μm/h growth rate using an Veeco Applied EPI nitrogen plasma source. Figure 1 shows the 2theta/omega x-ray diffraction spectra of our 0.37 μm AlN film on Z-cut lithium niobate. The dominant reflections present are the symmetric reflections of AlN and lithium niobate (LiNbO$_3$), indicating alignment of the (0001) direction of AlN along the (0001) direction of lithium niobate. The additional peak of lithium triniobate (LiNb$_3$O$_8$) was formed during the growth of AlN buffer layers at 800 °C. It is well known that the lithium triniobate phase forms on lithium niobate in the temperature range between 550 and 900 °C.[9] Three different thicknesses of AlN on lithium niobate were grown on lithium niobate resulting in progressive improvement in crystal quality with increasing thickness. The results of a 2theta/omega x-ray diffraction full width at half maxi-
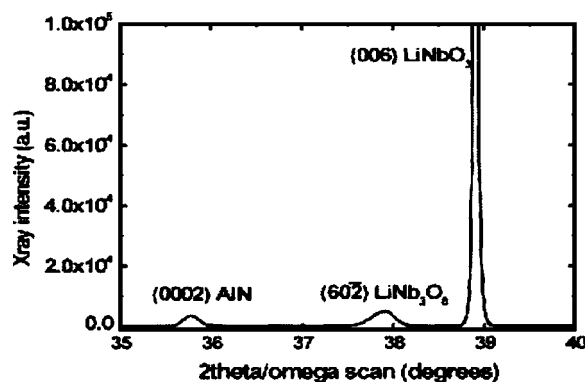
[a] On leave from Vilnius University, Department of Radiophysics, Vilnius, Lithuania.
[b] Author to whom correspondence should be addressed; electronic mail: shurm@rpi.edu

FIG. 1. X-ray diffraction spectra of AlN on lithium niobate.

TABLE I. Parameters of samples used in experiments.

Sample	AlN layer thickness, $h(\mu m)$	FWHM (arcsec) of ω-2θ
N1049	0.09	598
N1048	0.29	400
N1012	0.37	338

mum (FWHM) analysis correlating crystal quality with thickness are given in Table I. The detailed growth conditions can be found elsewhere.[10]

We have measured the SAW velocity and electromechanical coupling coefficient in the fabricated structures using the S-parameter method. Pure LiNbO$_3$ sample with no AlN layer was used for reference measurements. SAW interdigital transducers (IDT) with periodicity of 16 or 24 μm were deposited on the sample surface and their complex reflection coefficients S_{11} were measured with a network analyzer. An example of the Smith chart for SAWs propagating along the X axis of the substrate is shown in Fig. 2. The two characteristic loops with center frequencies near 240 and 276 MHz are observed at acoustic wavelength 16 μm. We attribute them to the excitation of Rayleigh wave and LSAW with the velocities 3840 and 4410 m/s, respectively. In the Y direction, we observed only one loop corresponding to the Rayleigh-type wave. These S_{11} parameter measurements are in keeping with what has been know for some time regarding the Z-cut of LiNbO$_3$.

Let us consider the propagation of surface acoustic waves in the structure consisting of a layer of thickness h deposited over the semi-infinite substrate. We use the method described in Ref. 11, which allows us to simulate both the Rayleigh-type and leaky surface acoustic waves. Let the SAW propagate along the x_1 direction in the plane normal to the x_3 axis. The propagation of elastic wave in the structure is described by Newton's law and Gauss' law for the electric field by

$$\rho \frac{\partial^2 u_j}{\partial t^2} - c_{ijkl}\frac{\partial^2 u_k}{\partial x_i \partial x_l} - e_{kij}\frac{\partial^2 \phi}{\partial x_i \partial x_k} = 0,$$

$$(1)$$

$$e_{ikl}\frac{\partial^2 u_k}{\partial x_i \partial x_l} - \varepsilon_{ik}\frac{\partial^2 \phi}{\partial x_i \partial x_k} = 0, \quad i,j,k,l = 1,2,3,$$

where ρ is the mass density of the material, c_{ijkl}, e_{ijk}, and ε_{ij} are the elastic stiffness, the piezoelectric, and the dielectric permittivity tensors, respectively, u_i is the particle displacement displacement vector, and ϕ is the electric potential. The displacement and electric potential are sought in the form of linear combinations of partial waves:

$$u_j = \left\{\sum_n \alpha_j^{(n)}\exp(-kb_j^{(n)}x_3)\right\}\exp[ik(lx_1 - Vt)],$$

$$j = 1,2,3,$$

$$(2)$$

$$\phi = \left\{\sum_n \alpha_4^{(n)}\exp(-kb_4^{(n)}x_3)\right\}\exp[ik(lx_1 - Vt)],$$

where $n=1,\ldots,4$ in the substrate and $n=5,\ldots,12$ in the layer, k and V are the acoustic wave number and phase velocity, respectively, $\alpha_j^{(n)}(j=1,2,3)$ are the coefficients one solves for to find the particle displacement field, $\alpha_4^{(n)}$ are the coefficients associated with the electrostatic potential, and l
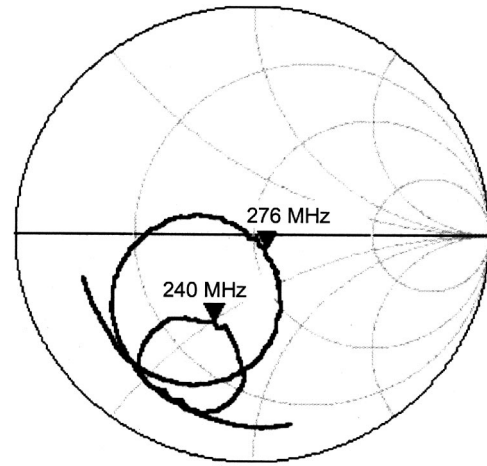

Freq (190.0 MHz to 320.0MHz)

FIG. 2. Smith chart of S_{11} parameter. Sample N1048: AlN layer thickness 0.29 μm; acoustic wavelength 16 μm, aperture length 0.5 mm, number of periods 70; SAW X-propagation.

$=1+i\delta$ with δ being the wave attenuation coefficient. For Rayleigh waves, where we assume there is no viscous loss, $\delta=0$, and the decay constants Re $b_j^{(n)}$ in the direction of depth of each subwave in the substrate are positive. For our coordinate system, we have $x_3=0$ at the surface and increasing as we move into the layer and substrate. For a leaky wave, δ is not 0, and at least one decay constant, Re $b_j^{(n)}$, in the substrate is negative, i.e., the relevant subwave grows in the direction of depth. This allows us to represent the particle displacement component associated with the leaky portion of the wave as increasing into the bulk. The phase velocity V and the decay constant l can be found by solving the system of equations (1) with the relevant boundary conditions. The electromechanical coupling coefficient is obtained from the well-known relation $K^2=2(V_f-V_m)/V_f$, where V_f and V_m are the SAW velocities on a free and electrically short-circuited surface, respectively. The material parameters used in the simulation are listed in Table II. For AlN, we used the elastic constants from Ref. 12, piezoelectric constants from Ref. 2, the dielectric permittivity from Ref. 13, and the mass density from Ref. 14. The corresponding parameters for LiNbO$_3$ were taken from Ref. 15.

The calculated attenuation of the X-propagating leaky wave, in the range of wavelengths and AlN layer thicknesses used in our experiment, is about 0.35 dB per wavelength for both free and metallized surface of AlN layer. The simulated dependencies of LSAW velocity and electromechanical coupling coefficient on the acoustic wave-number-layer thickness product, kh, are shown in Figs. 3 and 4, respectively.

TABLE II. Elastic stiffness constants (GPa), mass densities (10^3 kg/m^3), piezoelectric constants e_{ij}(C/m^2), and dielectric permittivities $\varepsilon_{ij}(10^{-11}$ F/m) used for calculations.

	c_{11}	c_{12}	c_{13}	c_{33}	c_{44}	c_{14}	ρ
LiNbO$_3$	203	53	75	245	60	9	4.7
AlN	410	140	100	390	121		3.26

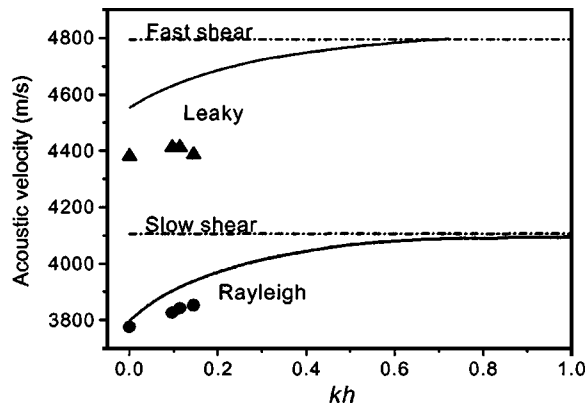|	e_{15}	e_{22}	e_{31}	e_{33}	ε_{11}	ε_{33}
LiNbO$_3$	3.7	2.5	0.2	1.3	38.9	25.7
AlN	−0.29		−0.58	1.39	7.53	7.53

FIG. 3. Velocities of leaky and Rayleigh-type surface acoustic waves propagating in AlN-on- Z-LiNbO₃ along substrate *X* axis. Dots, experiment: Rayleigh waves, circles; LSAW, triangles; lines, simulation. Horizontal lines: calculated velocities of shear bulk acoustic waves along the *X* axis of LiNbO₃.

The corresponding dependencies for the Rayleigh-type wave are shown for comparison. In Fig. 3, we also show the velocities of slow and fast shear bulk waves in LiNbO₃ substrate. The leaky wave velocity is in between those of the shear waves. The simulation predicts for the leaky wave a much higher velocity and K^2 values than for the Rayleigh wave.

To obtain the experimental values of the SAW velocity *V* and electromechanical coupling coefficient K^2, the transducer impedance *Z* was extracted from S_{11} measurements and calculated using the equivalent circuit mode.[16] By fitting the calculated real and imaginary parts of the impedance to the measured ones, the *V* and K^2 values were determined and plotted in Figs. 3 and 4, respectively. Details of their evaluation procedure can be found elsewhere.[2]

The measured LSAW velocity is about 4400 m/s in the entire range of experimental *kh* values. This is on average 15% higher than the Rayleigh wave velocities. The disagreement (about 4%) in simulated and measured numerical LSAW velocity values for pure LiNbO₃ can be attributed to the influence of IDT metal film (via the mass loading and electrical short-circuiting) and to possible small deviations of actual material tensors from the ones used in our calculations. The change in the substrate elastic properties due to

the formation of lithium triniobate phase during layer fabrication might be responsible for reduction of the velocity growth with *kh*, which was predicted by the simulation. The measured leaky wave k^2 values are on average about four times lower than the simulated ones, yet they are still advantageous compared to those of the Rayleigh wave (which has a particularly weak coupling constant for this orientation). It should be noted that the experimental values of K^2 might be underestimated due to the strong attenuation of leaky wave, which was not accounted for during the parameter extraction.

Finally, we have measured the temperature coefficient of frequency (TCF) defined as the relative shift of transducer center frequency with temperature:

$$\text{TCF} = \frac{1}{f_0}\frac{df_0}{dT}. \tag{3}$$

For the LSAW at $kh=0.1$, the slight improvement in the TCF value from -99 to -85 ppm/K was observed.

In conclusion, we have studied, by numerical simulation and experimental measurements, the propagation properties of leaky surface acoustic waves in MBE grown AlN layer on Z-cut LiNbO₃ structures. With *kh* in the range of $0-0.145$, the measured velocity of LSAW propagating along the *X* axis of the substrate was practically constant. Its value 4.4 km/s was slightly lower than the simulation-predicted values, which grew up with *kh* from 4.55 to 4.66 km/s. Changes in the LiNbO₃ substrate properties during the AlN layer deposition might be responsible for this deviation. The measured electromechanical coupling coefficients for LSAW are four times lower than the simulated values varying between 5.7% for pure LiNbO₃ and 2.7% for $kh=0.145$. This disagreement is attributed to the influence of strong LSAW attenuation. The thin AlN film slightly improved the measured temperature coefficient of frequency for LSAW as compared to that of the LiNbO₃ substrate.
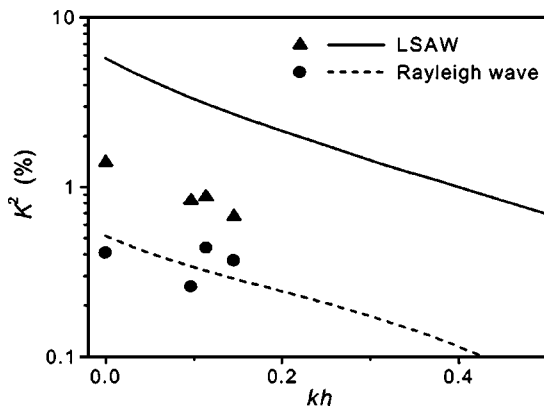

FIG. 4. Electromechanical coupling coefficients for leaky and Rayleigh SAWs propagating in AlN-on- Z-LiNbO₃ along substrate *X* axis. Dots, experiment; lines, simulation.

[1]G. Bu, D. Ciplys, M. Shur, L. J. Schowalter, S. Schujman, and R. Gaska, Electron. Lett. **39**, 755 (2003).
[2]G. Bu, D. Ciplys, M. Shur, L. J. Schowalter, S. Schujman, and R. Gaska, Appl. Phys. Lett. **84**, 4611 (2004).
[3]K. S. Kno, C.-C. Cheng, and Y.-C. Chen, IEEE Trans. Ultrason. Ferroelectr. Freq. Control **49**, 345 (2002).
[4]K. S. Kao, C. C. Cheng, Y. C. Chen, and Y. H. Lee, Appl. Phys. A: Mater. Sci. Process. **76**, 1125 (2003).
[5]S. Wu, Y.-C. Chen, and Y. S. Chang, Jpn. J. Appl. Phys., Part 1 **41**, 4605 (2002).
[6]S. Wu, Y.-C. Chen, and M.-S. Lee, J. Electron. Mater. **32**, 191 (2003).
[7]Y. Jin and S. G. Joshi, IEEE Trans. Ultrason. Ferroelectr. Freq. Control **43**, 491 (1996).
[8]I. E. Kuznetsova, B. D. Zaitsev, S. G. Joshi, and I. A. Borodina, IEEE Trans. Ultrason. Ferroelectr. Freq. Control **48**, 322 (2001).
[9]A. M. Prokhoov and Y. S. Kuz'minov, *Physics and Chemistry of Crystalline Lithium Niobate* (Hilger, New York, 1990).
[10]W. A. Doolittle, C. Namkoong, A. Carver, W. Henderson, D. Jundt, and A. S. Brown, Mater. Res. Soc. Symp. Proc. **743**, L1.4 (2002).
[11]K. Yamannouchi and K. Shibayama, J. Appl. Phys. **43**, 856 (1972).
[12]C. Deger, E. Born, H. Angerer, O. Ambacher, M. Stutzmann, J. Hornsteiner, E. Riha, and C. Fischerauer, Appl. Phys. Lett. **72**, 2400 (1998).
[13]A. J. Noreika, M. H. Francombe, and S. A. Zeitman, J. Vac. Sci. Technol. **6**, 194 (1969).
[14]G. A. Slack and T. F. McNelly, J. Cryst. Growth **34**, 263 (1976).
[15]D. Royer and E. Dieulesaint, *Elastic Waves in Solids* (Springer, Berlin, 1996), Vol. 1.
[16]R. Smith, H. M. Gerard, J. H. Collins, T. M. Reeder, and H. J. Shaw, IEEE Trans. Microwave Theory Tech. **17**, 856 (1969).